Contents lists available at ScienceDirect

Comptes Rendus Physique

www.sciencedirect.com

Spatial Atomic Layer Deposition (SALD), an emerging tool for energy materials. Application to new-generation photovoltaic devices and transparent conductive materials

Dépôt spatial par couche atomique : un outil émergeant pour les matériaux pour l'énergie. Application aux composants photovoltaïques de nouvelle génération et aux matériaux transparents et conducteurs

David Muñoz-Rojas *, Viet Huong Nguyen, César Masse de la Huerta, Sara Aghazadehchors, Carmen Jiménez, Daniel Bellet

Laboratoire des matériaux et du génie physique (LMGP), UMR 5628 CNRS – Grenoble INP Minatec, 3, parvis Louis-Néel, MINATEC CS 50257, 38016 Grenoble cedex 1, France

A B S T R A C T

Materials properties are the keystone of functional devices for energy including energy conversion, harvesting or storage. But to market new energy materials, the development of suitable processing methods allowing affordable prices is needed. Recently, a new approach to atomic layer deposition (ALD) has gained much momentum. This alternative approach is based on separating the precursors in space rather than in time, and has therefore been called Spatial ALD (SALD). With SALD, the purge steps typical of ALD are not needed and thus deposition rates a hundred times faster are achievable. Additionally, SALD can be easily performed at ambient atmosphere, thus it is easier and cheaper to scale up than conventional ALD. This opens the door to widespread industrial application of ALD for the deposition of energy materials for applications including solar energy, energy storage, or smart windows. SALD is presented here and examples of application to photovoltaics and transparent conductive materials are given. We show that SALD is capable of producing high-quality films fully suited for device integration.

© 2017 Académie des sciences. Published by Elsevier Masson SAS. All rights reserved.

R É S U M É

Les propriétés des matériaux constituent la pierre angulaire des dispositifs fonctionnels pour l'énergie, et cela concerne aussi bien la conversion, la récupération ou le stockage d'énergie. De façon à concevoir et fabriquer des nouveaux matériaux pour l'énergie à l'échelle industrielle, il est nécessaire de développer des méthodes de dépôt appropriées et accessibles à des prix abordables. Au cours des dernières années, une nouvelle approche du dépôt par couche atomique (ALD) a suscité un intérêt croissant. Cette approche repose sur la séparation des précurseurs dans l'espace plutôt que dans le temps lors du dépôt

* Corresponding author.
   E-mail address: david-munoz-rojas@grenoble-inp.fr (D. Muñoz-Rojas).

par couches atomiques, et a donc été appelée *Spatial ALD* (SALD). La méthode SALD permet d'éviter les étapes de purge typiques de l'ALD, et, par conséquent, les taux de dépôt de couches sont bien plus rapides, jusqu'à deux ordres de grandeur. De plus, le dépôt par SALD peut être facilement effectué à l'atmosphère ambiante. La mise en œuvre du SALD est donc plus facile et moins coûteuse que celle de l'ALD conventionnelle, ouvrant ainsi la possibilité de son application industrielle au dépôt de matériaux pour l'énergie, et notamment à des domaines tels que l'énergie solaire, le stockage énergétique ou les fenêtres intelligentes. Nous présentons ici la description de la méthode de dépôt SALD et l'illustrons avec des exemples appliqués au photovoltaïque et aux matériaux conducteurs transparents. Nous montrons notamment que la SALD est capable de produire des couches minces de la même qualité que par ALD classique, et qu'elle est donc parfaitement adaptée pour une intégration à l'échelle industrielle.

1. Introduction

Energy materials and energy devices, extremely relevant to our society, are specially concerned by phenomena taking place at the nanoscale, in particular at the interfaces and surfaces. For example, many photovoltaic technologies require the use of interface layers in order to maximise efficiency by limiting recombination or by improving the quality of contacts and alignment of electronic levels [1–4]. In the field of rechargeable batteries, new materials with higher reduction potentials are being developed and again surface and interface nanoengineering plays a key role in the efficiency of the final devices [5]. Also in the same field, nanometric control of interfaces would allow the development of all-solid 3D batteries [6].

But, in order to benefit from the potential impact of such interfacial or superficial layers in the performance of energy devices, cheap and scalable processing techniques should be developed. In particular, the homogeneous deposition of such thin layers, with a high degree of control over thickness and material properties and with high throughput is required, but is very challenging for nanometre-thick films [7].

In recent years, a new deposition technology that allows open-air, fast deposition of high-quality nanometre-thick materials over large surfaces has undergone a strong development. The new technique is called Spatial Atomic Layer Deposition (SALD), and is a variant of conventional atomic layer deposition (ALD). It is compatible with roll-to-roll (R2R) and other open air thin film deposition methods. In the next section, a brief introduction to SALD and to its historical development is given. This is followed by several examples of utilisation of SALD for the deposition of active components for new-generation solar cells. Finally, the application of SALD to the deposition and surface engineering of transparent conductive materials (TCM) is detailed, knowing that TCM are used in different energy domains such as solar energy, smart windows, or light-emitting diodes (LEDs).

2. Spatial Atomic Layer Deposition

SALD is a particular case of ALD, which is in turn a particular case of Chemical Vapour Deposition (CVD). In CVD, precursors are injected in a chamber and the chemical reaction between the precursors is activated at the substrate (most commonly thermally or using plasma). CVD allows deposition of high-quality thin films, but because it is a process controlled by the diffusion of species, homogeneity over large areas or on high aspect ratio or complex substrates is an issue [8]. In ALD, precursors are injected sequentially, reacting one at a time with active sites on the substrate surface. The injection of precursors is separated by a purge step in order to prevent mixing and reaction of precursors in the gas phase. The reaction is thus surface-limited and self-terminating, yielding uniform deposition on virtually any sample. In addition, the nature of ALD precursors allows the deposition of high-quality materials at lower temperatures than with CVD, even near room temperature. Indeed, ALD growth takes place only in a particular temperature window, since at low temperatures, precursor molecules cannot be sufficiently activated or desorption can be too slow. Conversely, at high temperatures, precursors can decompose at the surface or even before reaching it, and desorption can be too fast during the purge step [9–11].

The ALD technique was patented in 1977 by T. Suntola [12]. In this first patent, both the temporal and spatial approaches were already proposed. In the former, precursors are injected in consecutive pulses separated by purge steps (and thus separated in time, as shown in Fig. 1). In the latter, precursors are supplied in different locations (thus separated in space, see Fig. 2), and it is the substrate (or injector) which moves from one location to another.

SALD is thus equivalent to ALD from a chemical point of view, and thus surface limited, self-terminating reactions take place. This ensures a very precise growth per cycle, the conformal coating of high aspect ratio features, and the deposition of high quality films at low temperatures (below 400 °C). But, in addition to retaining the unique assets of ALD, SALD can be up to two orders of magnitude faster. Finally, the possibility to perform SALD at atmospheric pressure (AP-SALD) makes it cheaper and easier to scale up since complex and expensive vacuum processing is not required. Despite being patented in 1983, it was not until 2008 that the first scientific article on SALD was published [13]. Since this publication interest around
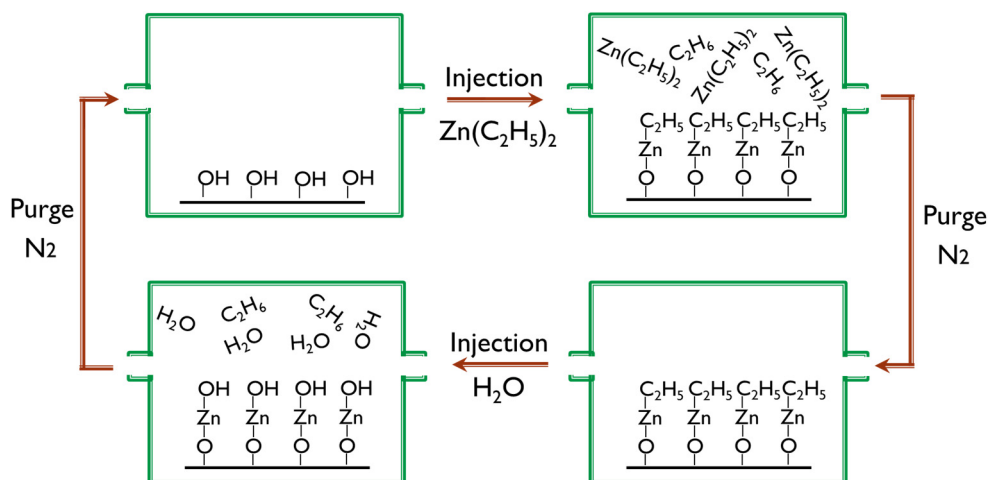
Fig. 1. Scheme of the Atomic Layer Deposition (ALD) process showing the alternative steps: a first precursor is injected and a purge occurs followed by the injection of the second precursor and so on.
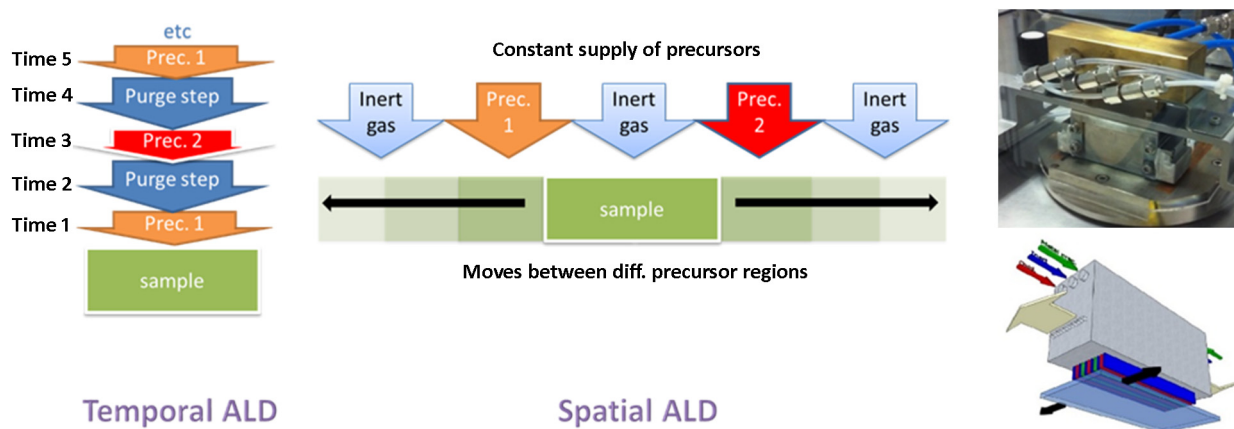

Fig. 2. Comparison between the temporal (and more traditional) ALD (left) and of SALD (middle): the separation between the two reactive precursors is performed either in time or in space, respectively. An image and a scheme of the deposition head used in our system are also presented (right). The green arrow and the channel represent the metallic precursor line, the blue ones represent the inert gas, and the red ones the oxidiser. The wide yellow arrows indicate the exit of the gasses from the head-carrying excess precursor and reaction by-products.

SALD has grown, with the associated increase in the number of publications involving SALD (both concerning development and applications), reaching more than 65 at present. In addition, and due to the suitability of the AP-SALD approach for industrial applications, many patents have been filled since 1983. In a patent by D. Levy (Kodak) dating from 2008 [14], an open-air close proximity reactor is proposed (see below). In a rather quick time, the technique has indeed reached industrial commercialisation and there are currently several companies developing, fabricating and/or selling SALD equipment, both for laboratory use and for industrial production. The spatial approach has proven to be a very versatile one from the engineering point of view, since many reactors have been reported to date [15,16]. SALD has also been referred to as continuous ALD since in most spatial ALD designs the precursors are being continuously fed into the reactor.

A very neat approach to AP-SALD was proposed in 2008 by Levy et al. from Kodak [13]. In their approach, an injector manifold head was designed, in which the different precursors were supplied along parallel channels kept away by adjacent inert gas-flow channels. By placing the substrate close enough to the deposition head, precursor separation is achieved with reasonable gas flows (up to thousands of sccm). A relative motion between substrate and head provides the ALD cycles yielding film growth (Fig. 3). As a result, the system is completely atmospheric and operates in the open air, without the use of a deposition chamber. In the initial Kodak model, the injector head was placed on top of the substrate. In a second model, the head was placed at the bottom with the outlets facing upwards and the substrate was oscillated on top of the head. Afterwards, other groups, including the "Laboratoire des matériaux et du génie physique" (LMGP) in Grenoble (France), have developed similar "close-proximity" approaches [17–19]. A.S. Yersak et al., for example, have taken advantage of the open air environment offered by this AP-SALD approach to implement the in-situ monitoring of film thickness. In that case, the substrate is scanned below the injection module and a reflectometer is placed in series to monitor film thickness [20].
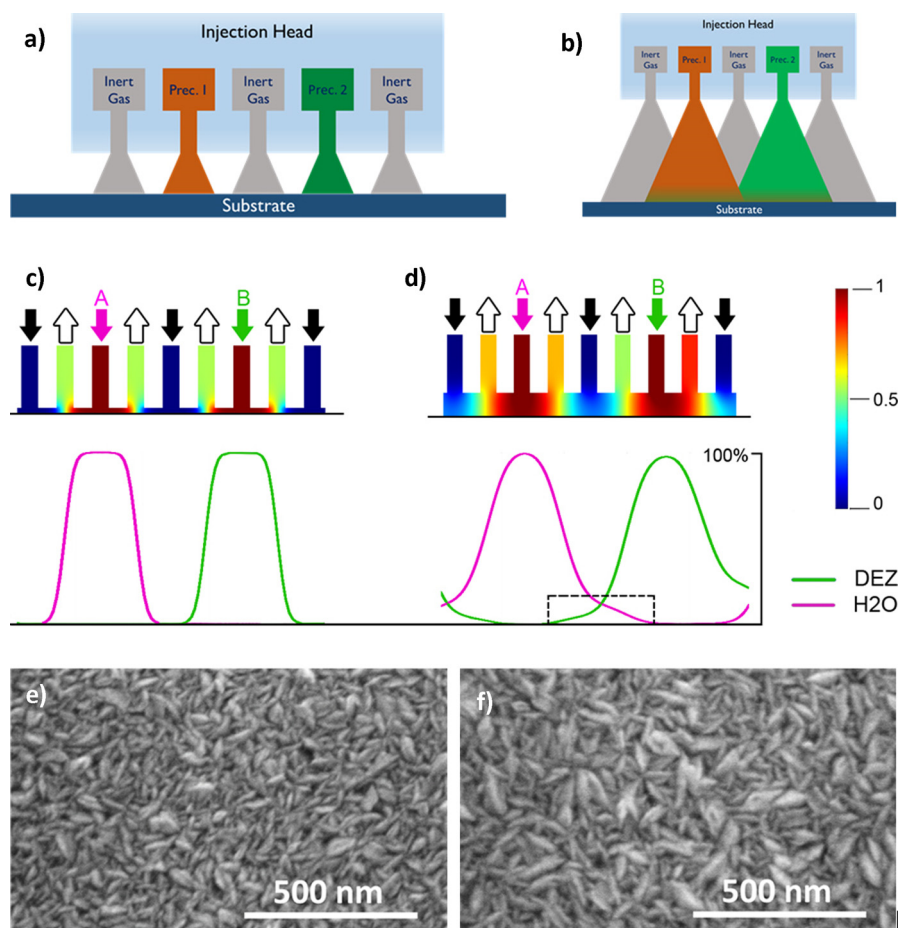
Fig. 3. The difference between SALD and CVD deposition modes. Scheme of the deposition head showing two precursor channels and different gaps between sample and head: a) small gap preventing mixing in the gas phase and b) large gap between head and sample yielding precursor mixing above the sample surface. c) and d) show a CFD stationary simulation of the two different modes. The simulation used a whole representation of the head to simulate the behaviour of the gases; here, for simplicity, only two precursor channels are shown. The inlets use a mass flow of 800 sccm, which is typically used in our system. The diffusion coefficient used is 10^{-5} m^2/s, which is the order of magnitude for a molecule in the gas phase [21]. A cross-section of the head with precursor, inert and evacuation channels is shown in which the normalised concentration of the different precursors is given by the colour scale to the right of the image. Below, normalised precursor concentration profiles calculated along the substrate line are shown. e) and f) show a SEM image of ZnO films deposited on Si with ALD and CVD modes in the same SALD reactor, respectively, showing a different morphology of the ZnO grains.

Another advantage of the close proximity approach based on a gas manifold, such as the ones in Fig. 2, is that it can be adjusted to switch between pure ALD mode and a more CVD-like mode. As already said, the close proximity between head and substrate prevents mixing of the different flows in the gap between the head and the substrate. Precursor concentration in the different flows must also be tuned to prevent diffusion of precursor molecules between the different channels. In such optimised conditions, ALD takes place, and reactions are limited to the surface and are self-terminating. But simply by increasing the gap between the head and the substrate, thanks to a mechanically controllable head-substrate assembly, the different precursors can meet in the gas phase above the substrate giving a CVD-like reaction mode (see scheme in Fig. 3). Although for complex samples with very high-aspect-ratio features CVD mode would not be desirable if a homogeneous coating were needed, for flat samples or samples not presenting complex features, going to CVD-like mode does not alter the quality of the material being deposited. And, in addition, faster deposition rates can be achieved since growth per cycle is larger with respect to the typical value for ALD conditions (using the same precursors and deposition temperature), given that the reaction is not limited to an adsorbed layer on the surface. Also important, because growth per cycle is still constant, the thickness of films deposited using CVD-like conditions can be controlled as precisely as when working in ALD conditions by simply adjusting the number of cycles used for deposition.

As in conventional ALD and CVD, modelling is an excellent tool to guide reactor design and for tuning the deposition conditions. We have used computational fluid dynamics (CFD) simulations (using COMSOL) to illustrate the difference between the ALD and CVD operation modes when using our SALD system. Figs. 3c and 3d show a flow simulation of a cross-section of the SALD head and the gap between the head and the substrate. The simulation uses two concentrated species to represent the precursor channels. The black lines at the bottom of the simulation image represent the position of the substrate.

Table 1

Comparative analysis between CVD (Chemical Vapour Deposition), ALD (Atomic layer Deposition) and AP-SALD (Atmospheric Pressure Spatial Atomic Layer Deposition).

	Key features	Advantages	Drawbacks	Examples of applications linked with energy
ALD	Separation of precursors in time. Typical growth rate: 0.01–0.1 nm/s.	Very conformal deposition even on high-aspect ratio features. Method very well adapted to deposit very well controlled film thickness (5–20 nm).	Slow deposition process. More efficient in vacuum. Suitable substrate needed. Less precursors available than for CVD.	Deposition of diffusion barrier for solid oxide fuel cell (SOFC), Encapsulation (OLEDS), blocking/selective layers (photovoltaics)...
AP-SALD	Spatial separation of precursors. Typical growth rate: 1–10 nm/s.	Very conformal, fast deposition. No vacuum needed. High throughput deposition. Compatible with other atmospheric deposition methods. High versatile in terms of reactor design.	Potential sensitivity to ambient oxygen/water when processing in air. High volatility precursors needed. Number of available precursors still limited.	Passivation layers for Si solar cells. Active layers in new generation solar cells. Surface engineering of transparent conductive materials. Deposition of multilayers...
CVD	Mixture of precursors. Typical growth rate: 0.5–10 nm/s. Deposition at high temperature, i.e. >300 °C (except for plasma enhanced CVD or UV assisted CVD).	Widely used in industry. Strong knowledge acquired over decades of use. Many precursors available.	Not suitable for very thin films. Not very suitable for polymeric substrates. Conformity on very high aspect-ratio features not possible.	CVD growth of electrodes for supercapacitors. Deposition of thin films for electrochromic oxides for smart windows, deposition of materials for lithium ion battery anodes, deposition of amorphous and polycrystalline Si...

Only two precursor channels (labelled A and B) have been modelled. The precursor channels are separated by three inert gas channels (indicated by black arrows) and by four evacuation channels (empty arrows). In Fig. 3c, the gap between the outlet of the head and the substrate is only 150 μm and the simulation shows that no precursor mixing takes place in the gas phase (shown by the dark blue colour of the region below the middle inert gas channel). Furthermore, a precursor concentration profile was plotted measuring the concentration at the line of the substrate, and is presented below the cross-section of the head. This plot also clearly confirms that precursors are confined to separated locations below the head. Conversely, in Fig. 3d the gap used for the simulation is 700 μm. In this case, precursor mixture in the gap is clearly obtained (see light blue colour below the middle inert gas channel). In the corresponding concentration profile, an overlap is clearly observed within the dotted box, indicating mixture of the precursors and thus yielding CVD-like conditions. Fig. 3e and f show SEM images of ZnO films deposited in the same conditions, but with different gaps (150 μm vs. 450 μm). The films were grown on Si substrates and the thickness values obtained were 170 and 217 nm, respectively. As shown in the images, apart from thickness, the morphology of the deposited films can be different between ALD and CVD modes.

The possibility of using CVD conditions with a close-proximity SALD equipment has already been exploited by R. Hoye et al. to deposit Mg-doped ZnO functional thin films [22]. Their report shows that high-quality multicomponent oxides can be deposited with much faster rates than with conventional ALD, at low temperatures. In addition, a model relating the composition of a target ternary oxide with the bubbling rates through the precursor bubblers is proposed. The quality of films deposited in CVD mode was evaluated by applying them in hybrid solar cells, in combination with poly(3-hexylthiophene-2,5-diyl) (P3HT). By controlling the Mg content, the open-circuit voltage of the devices could be increased over 100%.

K. Musselman et al. have also shown that SALD can be used in CVD mode even for coating high-aspect ratio features such as electrodeposited ZnO nanorods [23]. In their report, it is shown how a 15-nm-thick conformal Al_2O_3 coating was deposited by performing 40 cycles of SALD in ALD mode, taking 24 minutes. This gave a growth rate of 0.10 nm·cycle^{-1}, similar to what is found in conventional ALD. When CVD-like mode was tested on the same nanorods, 60 cycles were deposited in only 3 minutes, yielding uniform, crack and pinhole-free, conformal coatings 25 nm thick. This again gives a growth per cycle of 0.10 nm, which implies that, despite using faster CVD-like conditions, the reaction is still surface-limited as in ALD. These results show that the type of growth is also a function of the surface to be coated, in addition to sample–head distance and precursor flows. Therefore, a systematic study is required for each system and sample to assess the particular set of conditions (temperature, head-substrate distance, oscillation speed, etc.) in which pure ALD growth takes place. As explained in the next section, conformal coating of ZnO nanorod arrays with SALD yielded photovoltaic devices with increased performance. So it is clear from the above that SALD offers not only faster deposition rates, but also ambient processing, tunability between different types of growth modes and a high versatility in terms of system design. Table 1 gives a comparison between CVD, ALD and SALD.

3. Applications of SALD for photovoltaic devices

The first paper on SALD in 2008, from Kodak [13], already described the deposition of ZnO and Al_2O_3 layers as components in thin-film transistors (TFTs), showing that SALD produces films of high quality and functional devices. The same

group has published different studies on this line, including the use of growth inhibitors for the deposition of patterned films [24–27].

But despite this initial publication, most SALD research and commercialisation involves applications energy, in particular photovoltaics. The group from TNO (Netherlands Organisation for Applied Scientific Research) used their rotary reactor to deposit Al_2O_3 passivation layers for silicon solar cells, and the good results prompted the creation of the spin-off companies Solaytec [28]. The same group has dedicated efforts to deposit transparent conductive oxides (TCO), which constitute a key component of solar cells and of other optoelectronic devices as shown below, as well as more complex oxides for application in photovoltaic devices [29–32]. Prof. Driscoll's group was the first group to apply the SALD technique for the deposition of active layers for new generation solar cells [33–37]. For example, D. Muñoz-Rojas et al. showed that a 15-nm-thick amorphous TiO_2 layer can act as an efficient hole blocking layer in bulk heterojunction solar cells [34]. But, in addition to the pure deposition of active or passive layers, Prof. Driscoll's group and collaborators in the University of Cambridge have taken advantage of the high throughput of SALD for the realisation of many fundamental studies on photovoltaic device physics. As illustrated above, SALD allows a much faster deposition of samples with different crystallinity and properties than ALD, thus providing large batches in short times to be used to study device physics and assess solar cells' efficiency quickly. These and other early applications of SALD for the deposition of active components for new-generation solar cells have been described in detail in a recent review [38].

More recently, the same group has studied the physics of hybrid solar cells, in particular charge recombination mechanisms, by building devices incorporating an energy cascading interlayer [36]. To do so, SALD has been used to deposit extremely thin Nb_2O_5 layers on top of previously deposited TiO_2 layers. Hybrid and quantum dot-based cells were made both with and without the Nb_2O_5 interface layer. The results showed that both types of devices had better performance with the Nb_2O_5 interlayer, in both cases due to a suppression of nongeminate recombination. As mentioned in the previous section, SALD has also been successfully used by K. P. Musselman et al. to coat high aspect-ratio features, yielding more efficient photovoltaic devices [23]. The authors used SALD to coat arrays of electrodeposited ZnO nanorods with Al_2O_3, Cu_2O and Mg or N doped ZnO, showing that complete and conformal coverage of the high-aspect-ratio nanorods could be achieved with the various coating materials using conditions that resulted in deposition rates similar to those observed in conventional ALD (AP-SALD), as well as faster AP-CVD conditions. For the $Zn_{1-x}Mg_xO$ coatings, strong photoluminescence quenching was observed, indicating a very efficient charge transfer between the coating and the nanorod core. ZnO, N-doped ZnO, and $Zn_{1-x}Mg_xO$ coatings were tested in prototype nanorod hybrid and colloidal quantum dot solar cells. The coatings improved the efficiency of the devices, thanks to a reduction in unwanted charge recombination at the nanorod–absorber interface, as well as the potential elimination of shunt pathways at the base of the nanorods. Finally, SALD has also been used to deposit or engineer emerging transparent conductive materials (TCM). Although photovoltaics are one of the main applications of TCMs, because they can be used and tuned for other applications, a more detailed description of the application of SALD to TCMs is given next.

4. Applications of SALD for transparent conductive materials

Transparent electrodes (TE) have lately attracted a growing interest thanks to their use in many applications concerned with energy (photovoltaics, lighting…), displays (touch screens…) as well as transparent heaters or smart windows [39–42]. Transparent electrodes are used, for instance, in optoelectronics devices, either to collect charges from nearby functional layers (solar cells) or to supply them with charge carriers (light-emitting diode displays), while allowing light either to enter or escape the device. Their main physical properties [43] concern optical transparency, electrical conductivity (often measured through their sheet resistance), but other properties can also play a key role, such as haziness, for instance [44]. The need to reduce the cost of solar cells leads to use lower amounts of material and/or to improve efficiency, and/or to use less expensive deposition methods. This last constraint leads us, for instance, to use more vacuum-free methods and to avoid high-temperature treatments. As well, the use of polymeric substrates is attractive, since it would open new opportunities compatible with flexible electronics and with roll-to-roll technology. The latter would allow to fabricate thin films with the following interesting assets: high throughput, easy upscaling, and low cost. The main characteristics of SALD are for instance fully compatible with roll-to-roll technology. We will focus below on two materials that exhibit interests when used as transparent electrodes in solar cells: aluminium-doped ZnO and metallic nanowire networks.

In the current photovoltaic industry, the most commonly used transparent conductive material is still indium tin oxide (ITO), which has excellent electrical and optical properties, but also exhibits the following drawbacks: a rather high cost, indium scarcity and brittleness. From a technology point of view, crystalline silicon has been dominating the solar module industry, being used for over 90% of PV installations. Among different PV technologies, silicon heterojunction (HET) solar cells remains a hot topic in silicon PV research because of its record-efficiency energy conversion up to 26.6% [45]. Towards a sustainable development of high-efficiency and low-cost silicon solar cells, our research focuses on developing aluminium-doped zinc oxide (AZO) thin film, as an alternative for ITO, using SALD. The optimisation of AZO films prepared by our home-made SALD system shows that the crystallographic film texture moves from the *c*-axis (002) orientation to (100) orientation with increasing aluminium doping up to 2.33%, as shown in Fig. 4a. A shift of the (002) peaks to higher angles (2θ from 34.37° to 34.46°) is observed for samples oriented along (002). This can be explained by a decrease in the lattice along c when Al^{3+} ions replace Zn^{2+} ions in the ZnO lattice [19].
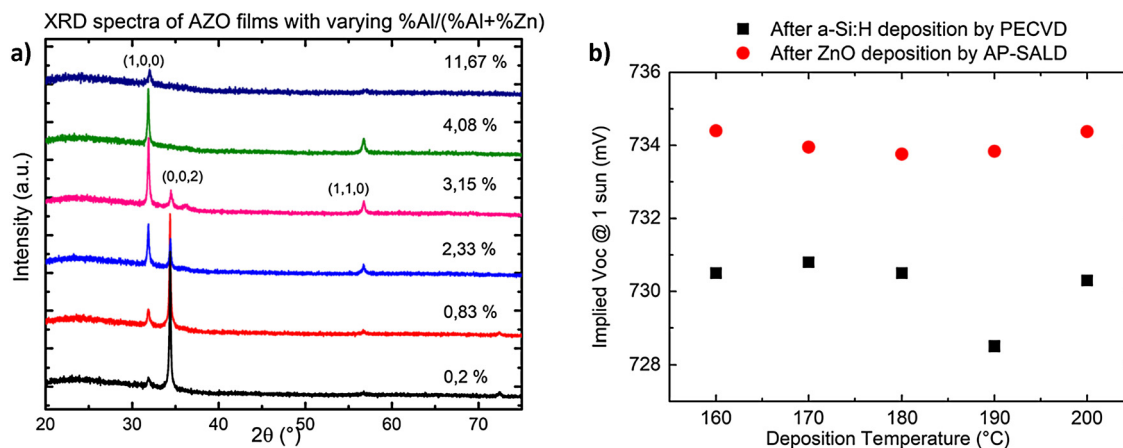
Fig. 4. a) X-ray diffraction patterns of AZO films deposited at 200 °C with varying aluminium doping. b) Implied open-circuit voltage at 1 sun of HET-like structure before and after ZnO deposition by AP-SALD versus deposition temperature. Reproduced with permission from ref. [19].

By adjusting the H_2O/metal precursor ratio and increasing the flowrates injected through the output channels of the SALD injector, the carrier concentration to increased from $1.01 \cdot 10^{20}$ cm^{-3} to $7.54 \cdot 10^{20}$ cm^{-3} corresponding to Al contents in the AZO films from 0.24% to 3%. This is accompanied by an increase in optical band gap from 3.3 eV to 3.6 eV, which is a typical behaviour of a degenerated semiconductor such as AZO. On the other hand, the carrier's mobility decreases while increasing the Al content in the films, which is mainly attributed to impurity scattering. This leads to a trade-off between mobility and carrier concentration, giving the lowest resistivity of $5.57 \cdot 10^{-3}$ $\Omega \cdot$cm, reached with an Al content of 1.19% [19].

The compatibility of SALD processing with HET cells was checked by depositing ZnO layers at 200 °C and studying the effect on the *a*-Si/*c*-Si interface. The recombination loss of photogenerated carriers is evaluated by using Quasi-Steady-State Photoconductance (QSSPC) lifetime measurements. In fact, the QSSPC measures the excess carrier density generated under one sun illumination in open circuit condition, from which the separation of two Fermi levels at the edges of the depletion region (also called implied-V_{oc}) is calculated. Fig. 4b shows an increase in the implied V_{oc} measured at one sun of a HET-like structure before and after ZnO deposition versus deposition temperature. This means that SALD processing can even reduce the recombination losses and so improve the passivation quality of *a*-Si/*c*-Si interface in HET cells, which is not the case of ITO deposition by sputtering [46]. Our ongoing study focuses on improving the conductivity of AZO films but this initial result demonstrates that SALD is a promising technique for processing HET cells and other sensitive devices.

Another candidate for transparent electrode are metallic nanowires (MNW). When MNWs are assembled into random percolating networks, the latter can indeed act efficiently as transparent electrodes [47,48], exhibiting an optical transparency of 89.2% and a sheet resistance lower than 3 Ω/sq [49]. Therefore they constitute a serious alternative to the reference material ITO. Such alternatives could be prepared by cost-effective and scalable processes (wet chemical synthesis, followed by large-area coating or printing at atmospheric pressure), and they can be easily integrated into flexible devices such as OLEDs or OPV due to their outstanding physical properties (optical, electrical, mechanical...) [48]. However, a severe limitation of MNW networks is their lack of stability, either when subjected to an electrical current, such as in solar cell applications (electrical stability) [50] or when the temperature is too high (thermal stability) [51]. One way to enhance the stability of MNW network is to cover them in a very uniform way by a thin oxide layer (a few nanometres thick) to prevent atomic surface diffusion and then to avoid morphological instability. The oxide layer should be thin enough to avoid any additional optical absorption, but thick enough to act as an efficient diffusion barrier.

The Transmission Electron Microscopy image reported in Fig. 5a clearly reveals that Al_2O_3 coatings deposited by SALD are very conformal. The Al_2O_3 layer in the figure is about 10 nm. The very small Al_2O_3 layer thickness, in combination with the large optical bandgap of Al_2O_3 (>4 eV), induces a negligible decrease in optical transmittance (only 1%). Fig. 5b shows the in-situ dependence of the electrical resistance measured when applying an electrical ramp of 1 V·min^{-1} for both bare and coated AgNWs; this coating corresponds to 50-nm-thick Al_2O_3. The electrical resistance increases slightly when increasing the voltage thanks to the Joule effect. At low voltages, this phenomenon is reversible [52]. For larger voltages, the resistance increase is more pronounced up to a non-reversible deterioration of the network associated with the divergence of the resistance. Fig. 5b clearly shows that this voltage failure occurs at larger voltage for the coated AgNWs (14 V) than for the bare ones (9 V). Therefore, the coating enhances the electrical stability (the same observation can be stated for thermal stability).

In conclusion, the atmospheric pressure spatial atomic layer deposition (AP-SALD) technique appears to drastically enhance the stability of AgNW networks thanks to a very conformal thin coating. The resulting physical properties of such thin oxide layers appear to make them very well suited to enhance the stability of MNW networks; this constitutes therefore an efficient method to better integrate MNW networks into solar cells. The nature of the deposited coating (for instance
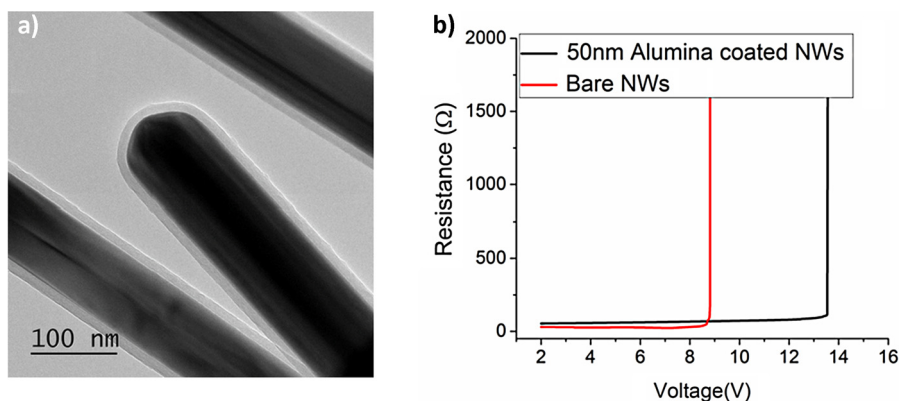
Fig. 5. a) Transmission Electron Microscopy image of silver nanowires (AgNW) coated with a thin Al_2O_3 layer deposited by Spatial ALD; b) Electrical resistance of a AgNW network measured *in situ* during a voltage ramp (1 V·min^{-1}) for either bare or coated AgNW with Al_2O_3 by SALD. A clear electrical stability enhancement is observed.

ZnO, Al_2O_3, TiO_2...) as well as its thickness should be optimised in order to reach better stability without degrading the collection of photo-generated carriers when such transparent electrodes are used in solar cells.

5. Some concluding remarks on SALD potential towards the energy domain and beyond

Although already patented in 1977 at the same time than temporal ALD, Spatial ALD has only been developed with the beginning of the 21st century. The possibility to perform ALD in at much faster deposition rate, at atmospheric pressure, and even in the open air has converted SALD into a technique that is gaining much attention and momentum, in particular in the field of renewable energies. Since the initial publications in 2008, the number of reports keeps increasing, with more than 65 papers at present. SALD has also made the transition from laboratory to industrial scale, and different commercial systems are already available both for laboratory and production scale. SALD is a very flexible deposition technology that allows a high degree of design freedom, as shown by the increasing number of reactors being developed.

Since in SALD the precursors are continuously being injected, an efficient separation by the inert gas flow/zone needs to be ensured. The analytical study of fluid dynamics and modelling are thus commonly used during the design of reactors and to evaluate optimum deposition conditions, as shown above and in several reports [53,54]. Many materials have been already deposited using SALD. Initial works focused on Al_2O_3 and ZnO. Later on, other binary oxides such as Cu_2O, TiO_2 or Nb_2O_5 have also been developed, together with the deposition of more complex oxides (including doping) and metals. Main applications of SALD to date have been for the deposition of components for TFTs, solar cells and LEDs and for the deposition of barrier and encapsulation layers. SALD has been demonstrated on flexible substrates such as paper or plastic and even on features with aspect ratio of 250. SALD has also been shown to offer the possibility of industrial nano-manufacturing of functional thin films, surpassing in capabilities other established techniques such as gravure printing, screen printing, knife-over-edge coating, slot-die coating, inkjet printing, spray deposition, as well as high-throughput sputtering and evaporation [55].

The combination of the unique assets of ALD with faster deposition rates and air processing, design flexibility and easy scalability are expected to make SALD one of the main thin film deposition techniques for energy materials in the coming years.

Acknowledgements

References

[1] R. Po, C. Carbonera, A. Bernardi, N. Camaioni, The role of buffer layers in polymer solar cells, Energy Environ. Sci. 4 (2011) 285–310, http://dx.doi.org/10.1039/c0ee00273a.

[2] R. Steim, F.R. Kogler, C.J. Brabec, Interface materials for organic solar cells, J. Mater. Chem. 20 (2010) 2499–2512, http://dx.doi.org/10.1039/b921624c.

[3] D. Muñoz, T. Desrues, P.J. Ribeyron, a-Si:H/c-Si Heterojunction solar cells: a smart choice for high efficiency solar cells, in: W.G.J.H.M. van Sark, L. Korte, F. Roca (Eds.), Physics and Technology of Amorphous–Crystalline Heterostructure Silicon Solar Cells, Springer-Verlag, Berlin, Heidelberg, 2012, pp. 549–572.

[4] A. Klein, C. Körber, A. Wachau, F. Säuberlich, Y. Gassenbauer, S.P. Harvey, D.E. Proffit, T.O. Mason, Transparent conducting oxides for photovoltaics: manipulation of Fermi level, work function and energy band alignment, Materials 3 (2010) 4892–4914, http://dx.doi.org/10.3390/ma3114892.

[5] S. Deng, B. Xiao, B. Wang, X. Li, K. Kaliyappan, Y. Zhao, Nano energy new insight into atomic-scale engineering of electrode surface for long-life and safe high voltage lithium ion cathodes, Nano Energy 38 (2017) 19–27, http://dx.doi.org/10.1016/j.nanoen.2017.05.007.

[6] V. Issue, A.C.S.A. Materials, A.C.S. Nano, Recent advances in atomic layer deposition, Chem. Mater. 28 (2016) 1943–1947, http://dx.doi.org/10.1021/acs.chemmater.6b00673.

[7] N.P. Dasgupta, L. Li, X. Sun, Atomic layer deposition of nanostructured materials for energy and environmental applications, Adv. Mater. 3 (2016) 1600914, http://dx.doi.org/10.1002/adma.201104129.

[8] A.C. Jones, M.L. Hitchman (Eds.), Chemical Vapour Deposition, Royal Society of Chemistry, Cambridge, ISBN 978-0-85404-465-8, 2008.

[9] M. Leskelä, M. Ritala, Atomic layer deposition (ALD): from precursors to thin film structures, Thin Solid Films 409 (2002) 138–146, http://dx.doi.org/10.1016/S0040-6090(02)00117-7.

[10] S.M. George, B. Yoon, A.A. Dameron, Surface chemistry for molecular layer deposition of organic and hybrid organic–inorganic polymers, Acc. Chem. Res. 42 (2009) 498–508.

[11] S.M. George, Atomic layer deposition: an overview, Chem. Rev. 110 (2010) 111–131, http://dx.doi.org/10.1021/cr900056b.

[12] T.S. Suntola, J. Antson, Method for producing compound thin films 1977, US Patent 4,058,430.

[13] D.H. Levy, D. Freeman, S.F. Nelson, P.J. Cowdery-Corvan, L.M. Irving, Stable ZnO thin film transistors by fast open air atomic layer deposition, Appl. Phys. Lett. 92 (2008) 192101, http://dx.doi.org/10.1063/1.2924768.

[14] D.H. Levy, Process for atomic layer deposition, US 7,413,982 B2, 2008.

[15] P. Poodt, D.C. Cameron, E. Dickey, S.M. George, V. Kuznetsov, G.N. Parsons, F. Roozeboom, G. Sundaram, A. Vermeer, Spatial atomic layer deposition: a route towards further industrialization of atomic layer deposition, J. Vac. Sci. Technol., A, Vac. Surf. Films 30 (2012) 010802, http://dx.doi.org/10.1116/1.3670745.

[16] D. Muñoz-Rojas, Dépôt par couche atomique spatiale (SALD), Techniques de l'Ingenieur (2016) 1–10.

[17] R. Chen, J.-L. Lin, W.-J. He, C.-L. Duan, Q. Peng, X.-L. Wang, B. Shan, Spatial atomic layer deposition of ZnO/TiO₂ nanolaminates, J. Vac. Sci. Technol., A, Vac. Surf. Films 34 (2016) 051502, http://dx.doi.org/10.1116/1.4955289.

[18] P. Ryan Fitzpatrick, Z.M. Gibbs, S.M. George, Evaluating operating conditions for continuous atmospheric atomic layer deposition using a multiple slit gas source head, J. Vac. Sci. Technol., A, Vac. Surf. Films 30 (2012) 01A136, http://dx.doi.org/10.1116/1.3664765.

[19] V.H. Nguyen, J. Resende, C. Jiménez, J. Deschanvres, P. Carroy, D. Muñoz, D. Bellet, D. Muñoz-Rojas, Deposition of ZnO based thin films by atmospheric pressure spatial atomic layer deposition for application in solar cells, J. Renew. Sustain. Energy 9 (2017) 021203, http://dx.doi.org/10.1063/1.4979822.

[20] A.S. Yersak, Y.C. Lee, J.A. Spencer, M.D. Groner, Atmospheric pressure spatial atomic layer deposition web coating with in situ monitoring of film thickness, J. Vac. Sci. Technol., A, Vac. Surf. Films 32 (2014) 01A130, http://dx.doi.org/10.1116/1.4850176.

[21] G.A. Lugg, Diffusion coefficients of some organic and other vapors in air, Anal. Chem. 40 (1968) 1072–1077, http://dx.doi.org/10.1021/ac60263a006.

[22] R.L.Z. Hoye, D. Muñoz-Rojas, K.P. Musselman, Y. Vaynzof, J.L. MacManus-Driscoll, Synthesis and modeling of uniform complex metal oxides by close-proximity atmospheric pressure chemical vapor deposition, ACS Appl. Mater. Interfaces 7 (20) (2015) 10684–10694, http://dx.doi.org/10.1021/am5073589.

[23] K.P. Musselman, D. Muñoz-Rojas, R.L.Z. Hoye, H. Sun, S.-L. Sahonta, E. Croft, M.L. Böhm, C. Ducati, J.L. MacManus-Driscoll, S. De Gendt, M. Heyns, M.M. Viitanen, M. de Ridder, H.H. Brongersma, Y. de Tamminga, T. Dao, T. de Win, M. Verheijen, M. Kaiser, M. Tuominen, Rapid open-air deposition of uniform, nanoscale, functional coatings on nanorod arrays, Nanoscale Horiz. 2 (2017) 110–117, http://dx.doi.org/10.1039/C6NH00197A.

[24] D.H. Levy, C.R. Ellinger, S.F. Nelson, Metal-oxide thin-film transistors patterned by printing, Appl. Phys. Lett. 103 (2013) 043505, http://dx.doi.org/10.1063/1.4816322.

[25] C.R. Ellinger, S.F. Nelson, Selective area spatial atomic layer deposition of ZnO, Al₂O₃, and aluminum-doped ZnO using poly(vinyl pyrrolidone), Chem. Mater. 26 (2014) 1514–1522, http://dx.doi.org/10.1021/cm402464z.

[26] C.R. Ellinger, S.F. Nelson, Design freedom in multilayer thin-film devices, ACS Appl. Mater. Interfaces 7 (2015) 4675–4684, http://dx.doi.org/10.1021/am508088p.

[27] S.F. Nelson, C.R. Ellinger, D.H. Levy, Improving yield and performance in ZnO thin-film transistors made using selective area deposition, ACS Appl. Mater. Interfaces 7 (2015) 2754–2759, http://dx.doi.org/10.1021/am5077638.

[28] P. Poodt, A. Lankhorst, F. Roozeboom, K. Spee, D. Maas, A. Vermeer, High-speed spatial atomic-layer deposition of aluminum oxide layers for solar cell passivation, Adv. Mater. 22 (2010) 3564–3567, http://dx.doi.org/10.1002/adma.201000766.

[29] A. Illiberi, P. Poodt, P.-J. Bolt, F. Roozeboom, Recent advances in atmospheric vapor-phase deposition of transparent and conductive zinc oxide, Chem. Vap. Depos. 20 (2014) 234–242, http://dx.doi.org/10.1002/cvde.201400056.

[30] A. Illiberi, R. Scherpenborg, F. Roozeboom, P. Poodt, Atmospheric spatial atomic layer deposition of in-doped ZnO, ECS J. Solid State Sci. Technol. 3 (2014) P111–P114, http://dx.doi.org/10.1149/2.002405jss.

[31] A. Illiberi, R. Scherpenborg, P. Poodt, F. Roozeboom, (Invited) spatial atomic layer deposition of transparent conductive oxides, ECS Trans. 58 (2013) 105–110, http://dx.doi.org/10.1149/05810.0105ecst.

[32] A. Illiberi, R. Scherpenborg, Y. Wu, F. Roozeboom, P. Poodt, Spatial atmospheric atomic layer deposition of Al$_x$Zn$_{1-x}$O, ACS Appl. Mater. Interfaces 5 (2013) 13124–13128, http://dx.doi.org/10.1021/am404137e.

[33] D. Muñoz-Rojas, M. Jordan, C. Yeoh, A.T. Marin, A. Kursumovic, L. Dunlop, D.C. Iza, A. Chen, H. Wang, J.L. MacManus-driscoll, Growth of 5 cm² V • 1s • 1 mobility, p-type copper (I) oxide (Cu₂O) films by fast atmospheric atomic layer deposition (AALD) at 225 °C and below, AIP Adv. 2 (2012) 042179, http://dx.doi.org/10.1063/1.4771681.

[34] D. Muñoz-Rojas, H. Sun, D.C. Iza, J. Weickert, L. Chen, H. Wang, L. Schmidt-Mende, J.L. MacManus-Driscoll, High-speed atmospheric atomic layer deposition of ultra thin amorphous TiO₂ blocking layers at 100 °C for inverted bulk heterojunction solar cells, Prog. Photovolt. 21 (2013) 393–400, http://dx.doi.org/10.1002/pip.2380.

[35] R.L.Z. Hoye, D. Muñoz-Rojas, D.C. Iza, K.P. Musselman, J.L. MacManus-Driscoll, High performance inverted bulk heterojunction solar cells by incorporation of dense, thin ZnO layers made using atmospheric atomic layer deposition, Sol. Energy Mater. Sol. Cells 116 (2013) 197–202, http://dx.doi.org/10.1016/j.solmat.2013.04.020.

[36] C.L. Armstrong, M.B. Price, D. Muñoz-Rojas, N.J.K.L. Davis, M. Abdi-Jalebi, R.H. Friend, N.C. Greenham, J.L. MacManus-Driscoll, M.L. Böhm, K.P. Musselman, Influence of an inorganic interlayer on exciton separation in hybrid solar cells, ACS Nano 9 (2015) 11863–11871, http://dx.doi.org/10.1021/acsnano.5b05934.

[37] A.T. Marin, D. Muñoz-Rojas, D.C. Iza, T. Gershon, K.P. Musselman, J.L. MacManus-Driscoll, Novel atmospheric growth technique to improve both light absorption and charge collection in ZnO/Cu$_2$O thin film solar cells, Adv. Funct. Mater. 23 (2013) 3413–3419, http://dx.doi.org/10.1002/adfm.201203243.

[38] D. Muñoz-Rojas, J. MacManus-Driscoll, Spatial atmospheric atomic layer deposition: a new laboratory and industrial tool for low-cost photovoltaics, Mater. Horizons 1 (2014) 314–320, http://dx.doi.org/10.1039/c3mh00136a.

[39] T. Minami, Transparent conducting oxide semiconductors for transparent electrodes, Semicond. Sci. Technol. 20 (2005) S35–S44, http://dx.doi.org/10.1088/0268-1242/20/4/004.

[40] K. Ellmer, Past achievements and future challenges in the development of optically transparent electrodes, Nat. Photonics 6 (2012) 809–817, http://dx.doi.org/10.1038/nphoton.2012.282.

[41] W. Cao, J. Li, H. Chen, J. Xue, Transparent electrodes for organic optoelectronic devices: a review, J. Photonics Energy 4 (2014) 040990, http://dx.doi.org/10.1117/1.JPE.4.040990.

[42] D.P. Langley, G. Giusti, M. Lagrange, R. Collins, C. Jiménez, Y. Bréchet, D. Bellet, Silver nanowire networks: physical properties and potential integration in solar cells, Sol. Energy Mater. Sol. Cells 125 (2014) 318–324, http://dx.doi.org/10.1016/j.solmat.2013.09.015.

[43] K. Ellmer, Past achievements and future challenges in the development of optically transparent electrodes, Nat. Photonics 6 (2012) 808–816, http://dx.doi.org/10.1038/nphoton.2012.282.

[44] G. Giusti, V. Consonni, E. Puyoo, D. Bellet, High performance ZnO–SnO$_2$:F nanocomposite transparent electrodes for energy applications, ACS Appl. Mater. Interfaces 6 (2014) 14096–14107, http://dx.doi.org/10.1021/am5034473.

[45] K. Yoshikawa, et al., Silicon heterojunction solar cell with interdigitated back contacts for a photoconversion efficiency over 26%, Nat. Energy (2017) 17032.

[46] D. Zhang, A. Tavakoliyaraki, Y. Wu, R.A.C.M.M. van Swaaij, M. Zeman, Influence of ITO deposition and post annealing on HIT solar cell structures, Energy Proc. 8 (2011) 207–213, http://dx.doi.org/10.1016/j.egypro.2011.06.125.

[47] D.P. Langley, G. Giusti, C. Mayousse, C. Celle, D. Bellet, J.-P. Simonato, Flexible transparent conductive materials based on silver nanowire networks: a review, Nanotechnology 24 (2013) 452001, http://dx.doi.org/10.1088/0957-4484/24/45/452001.

[48] T. Sannicolo, M. Lagrange, A. Cabos, C. Celle, J. Simonato, D. Bellet, Metallic nanowire-based transparent electrodes for next generation flexible devices: a review, Small 12 (2016) 6052–6075, http://dx.doi.org/10.1002/smll.201602581.

[49] M. Lagrange, D.P. Langley, G. Giusti, C. Jiménez, Y. Bréchet, D. Bellet, Optimization of silver nanowire-based transparent electrodes: effects of density, size and thermal annealing, Nanoscale 7 (2015) 17410–17423, http://dx.doi.org/10.1039/c5nr04084a.

[50] H.H. Khaligh, I.A. Goldthorpe, Failure of silver nanowire transparent electrodes under current flow, Nanoscale Res. Lett. 8 (2013) 1–6.

[51] D.P. Langley, M. Lagrange, G. Giusti, C. Jiménez, Y. Bréchet, N.D. Nguyen, D. Bellet, Metallic nanowire networks: effects of thermal annealing on electrical resistance, Nanoscale 6 (2014) 13535–13543, http://dx.doi.org/10.1039/C4NR04151H.

[52] M. Lagrange, T. Sannicolo, D. Muñoz-Rojas, B.G. Lohan, A. Khan, M. Anikin, C. Jiménez, F. Bruckert, Y. Bréchet, D. Bellet, Understanding the mechanisms leading to failure in metallic nanowire-based transparent heaters, and solution for stability enhancement, Nanotechnology 28 (2017) 055709, http://dx.doi.org/10.1088/1361-6528/28/5/055709.

[53] D. Pan, T.-C. Jen, C. Yuan, Effects of gap size, temperature and pumping pressure on the fluid dynamics and chemical kinetics of in-line spatial atomic layer deposition of Al$_2$O$_3$, Int. J. Heat Mass Transf. 96 (2016) 189–198, http://dx.doi.org/10.1016/j.ijheatmasstransfer.2016.01.034.

[54] Z. Deng, W. He, C. Duan, R. Chen, B. Shan, Mechanistic modeling study on process optimization and precursor utilization with atmospheric spatial atomic layer deposition, J. Vac. Sci. Technol., A, Vac. Surf. Films 34 (2016) 01A108, http://dx.doi.org/10.1116/1.4932564.

[55] K.P. Musselman, C.F. Uzoma, M.S. Miller, Nanomanufacturing: high-throughput, cost-effective deposition of atomic scale thin films via atmospheric pressure spatial atomic layer deposition, Chem. Mater. 28 (2016) 8443–8452, http://dx.doi.org/10.1021/acs.chemmater.6b03077.